

## FLEXURAL VIBRATIONS OF A DOUBLE-LAYER ELASTIC PLATE

Narzullaev Muhammad Azamat,  
Doctoral Student Bukhara State Technical University (Uzbekistan)

A B S T R A C T	K E Y W O R D S
Consider a plate whose neutral plane coincides with the plane x, z, and the y coordinate coincides with the direction of thickness.	Analysis of numerical, material density, problem solving, harmonic wave, wave number, deformation, linear elasticity, isotropic material, algebraic equations, transcendental equation, Müller's method, Newton's method.

### Introduction

Consider a plate whose neutral plane coincides with the plane x, z, and the y coordinate coincides with the direction of thickness. Let harmonic bending waves propagate along the plate in the direction of the z axis.

The base material  $-\frac{b}{2} \leq y \leq \frac{b}{2}$  of the plate occupies a sphere, and the coating, each of which has the same thickness  $b/2$  everywhere, occupies the sphere  $(-n + b/2 \leq y \leq -h; h \leq y \leq b/2 + h)$ . Let  $G$ ,  $\mu$  and  $\rho$  denote the modulus of volumetric compression, the modulus of shear, and the density of the base layer material, respectively.

In this case, the solution of the Rayleigh-Lamb problem for the main layer is obtained using the variable separation method, and the displacements  $u$ ,  $v$ ,  $w$  (along the x, y, and z axes, respectively) in the propagation of a harmonic wave with a frequency and wave number  $k$  are of the form:

$$u = 0; \quad \vartheta = (\alpha A_1 \operatorname{ch} \alpha x_2 - k C_1 \operatorname{sh} \beta x_2) e^{i(\omega t - kz)},$$

$$w = (-ikA, \operatorname{ch} \alpha y + i\beta C_1 \operatorname{sh} \alpha y) e^{i(\omega t - kz)},$$

$-\frac{b}{2} \leq y \leq \frac{b}{2}$  for where  $A_1$  and  $S_1$  are constants, and the parameters are defined using the following  $\alpha$   $\beta$  expressions:

$$\alpha^2 = k^2 - \frac{\omega^2 \rho}{\lambda G + \frac{4}{3} \mu}; \quad \beta^2 = k^2 - \frac{\omega^2 \rho}{\mu}.$$

(1)

Based on the relationship between stresses and strains of the theory of linear elasticity for a homogeneous isotropic material

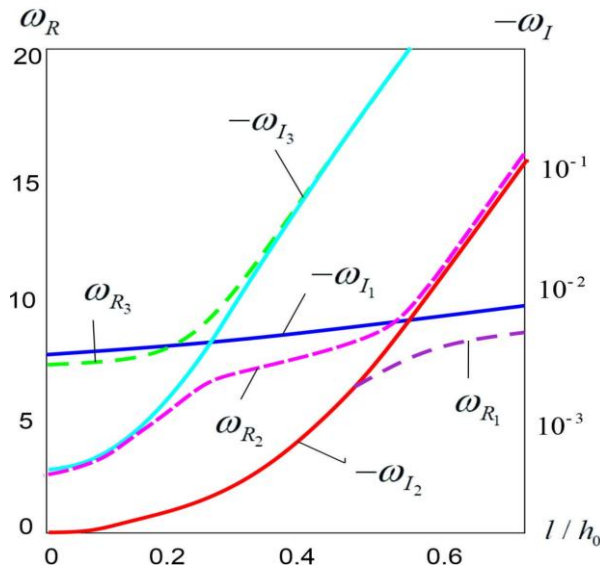


Figure 1. Change in frequency depending on the ratio of thicknesses of real and abstract parts

$$\sigma_{xz} = (G - 2/3\mu)A_1(\alpha^2 - k^2)sh\alpha y;$$

$$\sigma_{yy} = A_1[(G - 2/3\mu)(\alpha^2 - k^2) + 2\mu\alpha^2]sh\alpha y - 2\mu k\beta C_1 sh\beta y;$$

$$\sigma_{xy} = \sigma_{xx} = 0;$$

$$\sigma_{yz} = -2\mu i k A_1 \alpha c h x y + i \mu C_1 (k^2 + \beta^2) c h \beta y;$$

$$\sigma_{yy} = A_1[(G + 2/3\mu)(\alpha^2 - k^2) + 2\mu\alpha^2]sh\alpha y + 2\mu k\beta C_1 sh\beta y.$$

Expressions for moving points on the top outer layer that satisfy the equations of motion are generally as follows:

$$u=0;$$

$$\mathcal{G} = -\alpha c [\beta_1 sh\alpha_e(y-H) + F_1 ch\alpha_e(y-H)] + k [D_1 ch\beta_c(y-H) + M_1 sh\beta_c(y-H)]$$

$$w = ik [\beta_1 ch\alpha_e(y-H) + F_1 sh\alpha_e(y-H)] - i\beta_c [D_1 sh\beta_c(y-H) + M_1 ch\beta_c(y-H)]$$

Here, B1, D1, F1, M1 are constants,  $\alpha_c$  and the  $\beta_c$  parameters are defined from the following ratios, which are similar:

$$\alpha_c^2 = k^2 - \frac{\omega^2 \rho_c}{G_e + \frac{4}{3}\mu_c}; \quad \beta_c^2 = k^2 - \frac{\omega^2 \rho_c}{\mu_c},$$

Here, the c index refers to the characteristics of the coating material.  $-H = -(b_1 + b/2) \leq y \leq -h$

Using the antisymmetry property of a bending wave for a field, it is possible to measure the following families of bonds:

$$U(y) = u(-y); \quad \mathcal{G}(y) = \mathcal{G}(-y); \quad w(y) = -w(-y) \quad (2)$$

Taking into account the properties of solution (2), we will limit ourselves to considering the region below  $0 \leq y \leq H$ . The following boundary conditions must be met on a free surface  $y=H$ :

$$\sigma_{xy} = \sigma_{yy} = \sigma_{yz} = 0$$

In addition, the condition of continuity of displacements on the contact surface is  $y = b$

$$u(b^-) = u(b^+), \quad \vartheta(b^-) = \vartheta(b^+), \quad w(b^-) = w(b^+) \quad (3)$$

and the condition of equality:

$$\sigma_{xy}(b^-) = \sigma_{yy}(b^+), \quad \sigma_{yy}(b^-) = \sigma_{xy}(b^+), \quad \sigma_{yz}(b^-) = \sigma_{yz}(b^+)$$

where  $(b=b/2)$  must be satisfied. Based on conditions (1), (2), (3) and symmetry conditions, we construct a system of six homogeneous linear algebraic equations with respect to six invariants (A1, B1, C1, D1, F1, and M1). The first of these constants determines the deformation state of the base layer, the other four determine the deformation state of the top layer of the coating:

$$[C]\{q\} = \{0\}.$$

In order for a system of equations to have non-trivial solutions, the determinant of the matrix formed from the coefficients of the system must be equal to zero:

$$F(\Omega) = [C] = 0 \quad (4)$$

In here

$$\begin{aligned} C_{11} &= \alpha_c h \alpha_c k; C_{12} = -k c h \beta_c k; C_{13} = \alpha_c s h \alpha_c (b - H); \\ C_{14} &= \alpha_c c h \alpha_c (b - H); C_{15} = k c h \beta_c (b - H); \\ C_{16} &= -k s h \beta_c (b - H); C_{21} = -k s h \alpha_c b; C_{22} = \beta_c s h \beta_c h \\ C_{23} &= -k c h \alpha_c (b - H); C_{24} = -k c h \alpha_c (b - H); \\ C_{25} &= \beta_c s h \beta_c (b - H); C_{26} = \beta_c s h \beta_c (b - H); \\ C_{31} &= \alpha_1 s h \alpha_c b; C_{32} = -2 \mu_c k \beta_c s h \beta_c b \\ C_{33} &= -\alpha_2 c h \alpha_c (b - H); C_{34} = -\alpha_2 c h \alpha_c (b - H); \\ C_{35} &= 2 \mu_c k \beta_c s h \beta_c (b - H); C_{36} = 2 \mu_c k \beta_c c h \beta_c (b - H); \\ C_{41} &= -2 \mu_c k \alpha_c s h \alpha_c h; C_{42} = \mu_c \alpha_3 c h \beta_c h; \\ C_{43} &= -2 \mu_c k \alpha_c s h \alpha_c (b - H); C_{44} = -2 \mu_c k \alpha_c c h \alpha_c (b - H); \\ C_{45} &= \mu_c \alpha_1 c h \beta_c (b - H); C_{46} = \mu_c \alpha_1 s h \beta_c (b - H); \\ C_{51} &= C_{52} = C_{54} = C_{55} = 0; C_{53} = -\alpha_3; C_{56} = -2 \mu_c k \beta_c; \\ C_{61} &= C_{62} = C_{63} = C_{66} = 0; C_{64} = -2 \mu_c k \alpha_c; C_{65} = \mu_c \alpha_c; \end{aligned}$$

In here

$$\alpha_1 = G(k^2 - \alpha^2) - \frac{2}{3}\mu(k^2 + \alpha^2); \alpha_2 = k^2 + \alpha^2;$$

$$\alpha_3 = G(k^2 - \alpha_c^2) - \frac{2}{3}\mu_c(k^2 + 2\alpha_c^2); \alpha_4 = k^2 + \beta_c^2.$$

Transcendental equation (4) is solved numerically using the Müller method. Three methods can be used to solve the frequency transcendental equation (4):

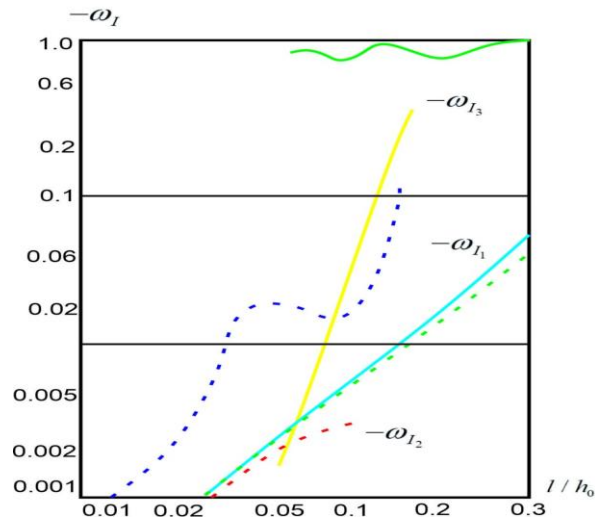


Figure 2. Frequency Change Depending on the Ratio of Thickness of Abstract Parts

- the solution of a system of two transcendental equations;
- direct complex roots using numerical methods (Müller's method, Newton's method and other methods);
- approximate solution of the frequency equation by the method of small parameters.

If  $F(\Omega)$  is the value of the determinant of equation (4), then equation (4) can be divided into two with extreme caution in interpreting the results.

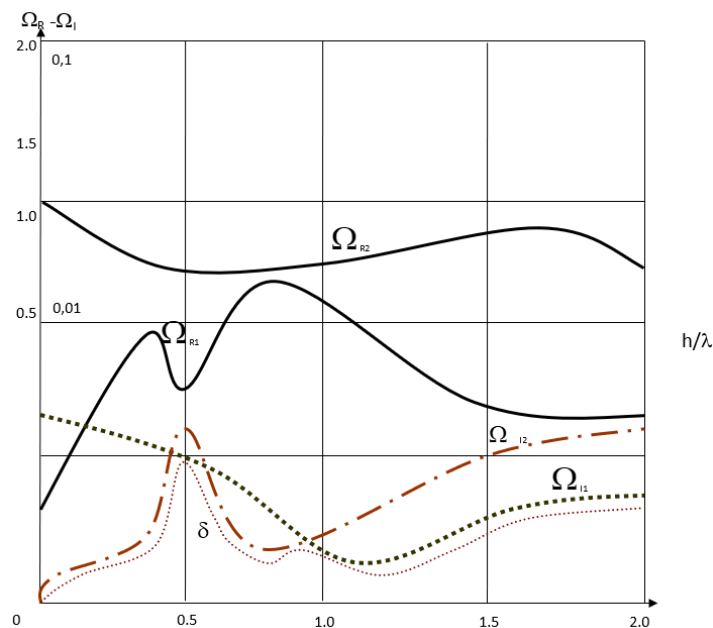


Figure 3. Change in natural frequency ( $\Omega R$ ) and attenuation coefficient as a function of wavelength

The frequency equation (4) is solved by the Müller method. In all cases, the Poisson's ratio is assumed to be 0.30 and 0.25 for the middle layer and the cover layer, respectively;  $C_{pc} = 5400$  m/s;  $S_c = 3195$

m/s;  $CL_{pk} = 2300$  m/s;  $C_{spk} = 2300$  m/s;  $h/b = 0.1$ ,  $\rho_{cp} = \frac{\rho_{pk}}{\rho_c} = 0.4452$  (ratio of coating to middle layer).

Rheological properties of the coating  $A = 0,048$ ;  $b = 0,05$ ;  $a = 0,1$ . The values given are valid for the middle layer of duralumin and for the acrylic coating.

The change in frequency depending on the ratio of the thickness of the abstract parts is shown in Figure 2. The shells are not elastic and diffusive. The filling of the cavity is elastic. In other words, the construction is dissipatively heterogeneous.

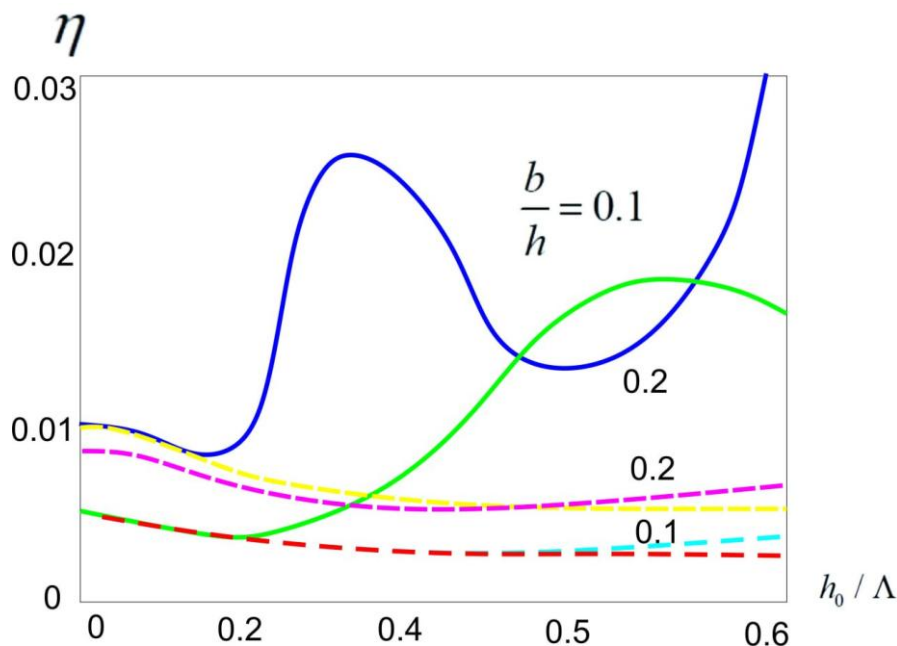


Figure 4. Change in Extinction Coefficient as a Function of Wavelength

The results are presented graphically as a real part of the frequency and the change in the loss coefficient (Potter's coefficient) relative to the dimensionless wave number (the ratio of the half-thickness of the layer of the medium to the wavelength). The absolute error of the eigenvalues in the

calculations was about the exact equations  $14 \cdot 10^{-6}$  of . Figure 3 shows the change in the real and abstract parts of the complex frequency relative to the dimensionless wavelength. In the case of dissipative inhomogeneous mechanical systems, a non-monotonic dependence of the attenuation coefficient on the wavelength was found. Here, the function of the global attenuation coefficient is performed by the abstract parts of the first and second natural frequencies. When these  $(\Omega Rk)$  frequencies converge, the intersection of the abstract parts of the first and second modes of natural frequencies is observed. A similar effect was observed in the work of Yu.N. Rabotnov. was also discovered when using a fractional-exponential nucleus

Graphs of dispersion curves,  $k^*$ , as well as their projections on the plane  $(\omega^*, k)$  for both positive and negative imaginary parts of  $k^*$  were considered. Projections of  $k^*$  on the plane  $(\omega^*, \alpha)$  for both positive

and negative real parts of  $k^*$  at different values of the parameters  $k$  were considered and  $\beta$  that represent the hereditary properties of the material.

Analysis of numerical solutions shows that the greater  $m$  or the lower the value of  $\beta$ , the earlier and more widely the variance curves  $k^*$  with the positive and negative imaginary parts begin to diverge. Numerical calculations show that with a decrease in the value of  $m$  or an increase in the value of  $\beta$ , the dispersion curves tend to become elastic. In addition, it has been established that the dispersion curves of the hereditary elastic spectrum, belonging to the elastic spectrum, consist of a complex number  $k^*$  with negative imaginary parts, which determines the attenuation of the solution by the coordinate.

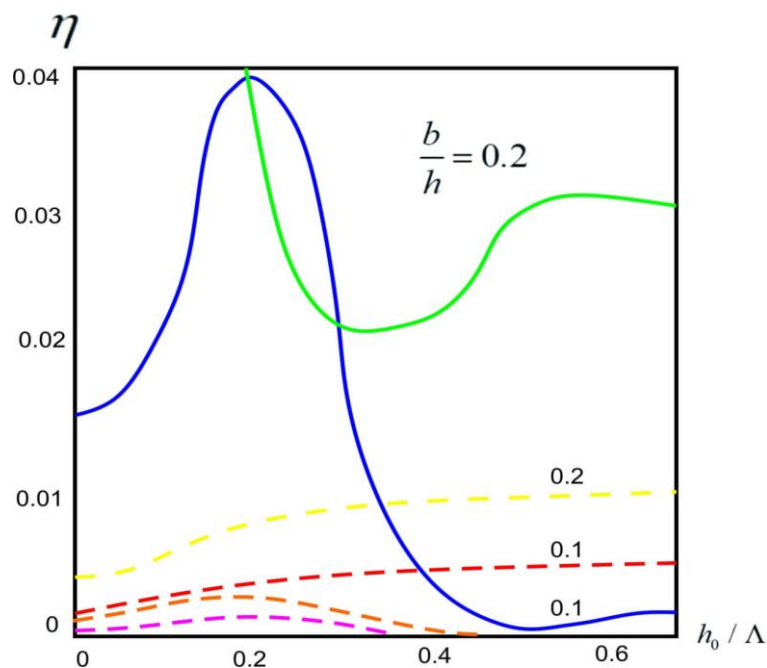


Figure 5. Change in Extinction Coefficient as a Function of Wavelength

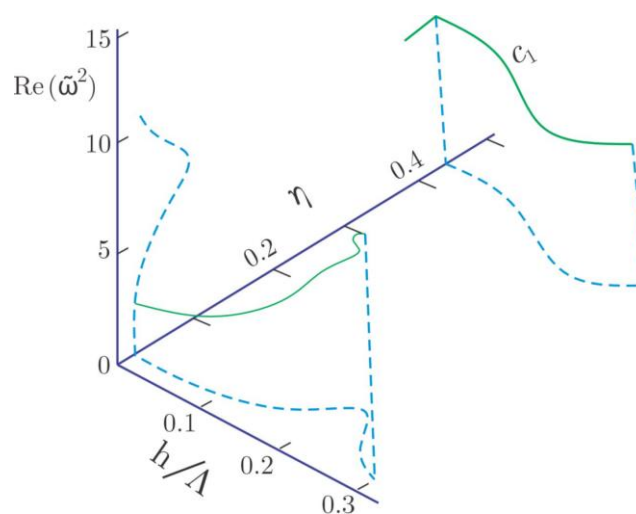


Figure 6. Change in Attenuation Coefficient and Actual Part of Frequency as a Function of Wavelength

Figures 5 and 4 show the change in the extinction coefficient as a function of wavelength. This is also obtained for a dissipative inhomogeneous mechanical system. The change in the attenuation coefficient and the actual part of the frequency as a function of the wavelength is shown in Figure 6. It should be noted that the concepts of "closing frequency" (locking frequency) ( $k^* = 0$ ,  $\omega^* > 0$ , since there are no roots of the dispersion equation) and "frequency minimum" (since  $\omega^*$  monotonically increases as you move along the network) lose their meaning for the genetic-elastic spectrum.

Analysis of the numerical results shows that elastic-elastic spectral networks have the greatest curvature around the closing frequencies and frequency minima in the elastic spectral network. An increase in  $m$  values, as well as a decrease in  $\beta$  values, leads to smoothing of dispersion curves in these regions.

Thus, for the elastic spectrum, the elastic spectrum is approximately the same as for the hereditary elastic spectrum,  $m \rightarrow 0$ ,

It can be considered asymptotic at  $\beta \gg 1$ .

Asymptotic roots for the first mode near zero frequency are obtained. For the symmetrical DKX case for the first mode, we get:

$$k_1 = c_{12}\omega + c_{13}\omega^{3/2} + O(\omega^2), \alpha_1 = d_{13}\omega^{3/2} + O(\omega^2)$$

where  $c_{12}$ ,  $c_{13}$ ,  $d_{13}$  are functions dependent on  $v$ ,  $m$ ,  $\beta$ .

It was shown that at  $m = 0$  these asymptotics overlap with similar asymptotics of the elastic layer. Numerical calculations show that numerical solutions and asymptotics overlap in the regions under consideration.

The analysis of dispersion equations and their numerical solutions allows us to draw the following conclusions:

- when replacing  $\tilde{k}$  with  $-\tilde{k}$  symmetry of dispersion curves is observed;
- the higher the value of  $m$  or the lower the value of  $\beta$ , the earlier and faster the dispersion curves with the positive and negative imaginary parts diverge;
- the higher the value of  $m$  and the lower the value of  $b$ , the faster the variance curve with positive and negative fractions;
- dispersion curves of the genetic-elastic spectrum, corresponding to the real grid of the elastic spectrum, consist of a complex number, the abstract part of which is positive, and this solution determines the inversion to zero of the coordinate;
- the concept of a closing frequency for the hereditary-elastic spectrum loses its meaning, since  $y = 0$  and  $\omega > 0$  will not be the roots of the dispersion equation;
- Networks of the hereditarily elastic spectrum have the greatest curvature near the closing frequency of the elastic spectrum. An increase in the values of  $m$ , as well as a decrease in the values of  $\beta$ , leads to smoothing of the dispersion curves in these regions.

Thus, the elastic spectrum can be considered asymptotic to the hereditary elastic spectrum at  $k \rightarrow 0$ ,  $\beta \gg 1$ .



## References

1. Cui, J.; Ye, R.; Zhao, N.; Wu, J.; Wang, M. Assessment on energy absorption of double layered and sandwich plates under ballistic impact. *Thin-Walled Struct.* 2018, 130, 520–534.
2. Tian, A.; Ye, R.; Ren, P.; Jiang, P.; Chen, Z.; Yin, X.; Zhao, Y. New higher- order models for sandwich plates with a flexible core and their accuracy assessment. *Int. J. Struct. Stab. Dyn.* 2019, 19, 1950024.
3. Zhao, N.; Ye, R.; Tian, A.; Cui, J.; Ren, P.; Wang, M. Experimental and numerical investigation on the anti- penetration performance of metallic sandwich plates for marine applications. *J. Sandw. Struct. Mater.* 2019. doi:10.1177/1099636219855335.
4. Kirchhoff, V.G. Uber das gleichgewicht und die bewegung einer elastischen scheibe. *J. Fur Die Reine Und Angew. Math.* 1850, 40, 51–88.
5. Mohammadi, M.; Saidi, A.R.; Jomehzadeh, E. Levy solution for buckling analysis of functionally graded rectangular plates. *Appl. Compos. Mater.* 2010, 17, 81–93.
6. Mindlin, R.D. Influence of rotatory inertia and shear on flexural motions of isotropic, elastic plates. *J. Appl. Mech.* 1951, 18, 31–38.
7. Ardestani, M.M.; Soltani, B.; Shams, S. Analysis of functionally graded stiffened plates based on FSDT utilizing reproducing kernel particle method. *Compos. Struct.* 2014.